Evidence for Symplastic Phloem Unloading in Sink Leaves of Barley[1]

Sophie Haupt, George H. Duncan, Steve Holzberg, and Karl J. Oparka*

Unit of Cell Biology, Scottish Crop Research Institute, Invergowrie, Dundee DD2 5DA, United Kingdom (S.H., G.H.D., K.J.O.); and Large Scale Biology Corporation, 3333 Vaca Valley, Vacaville, California 95688 (S.H.)

The pathway of phloem unloading in sink barley (*Hordeum vulgare*) leaves was studied using a combination of electron microscopy, carboxyfluorescein transport, and systemic movement of barley stripe mosaic virus expressing the green fluorescent protein. Studies of plasmodesmatal frequencies between the phloem and mesophyll indicated a symplastic sieve element- (SE) unloading pathway involving thick-walled and thin-walled SEs. Phloem-translocated carboxyfluorescein was unloaded rapidly from major longitudinal veins and entered the mesophyll cells of sink leaves. Unloading was "patchy" along the length of a vein, indicating that sieve element unloading may be discontinuous along a single vascular bundle. This pattern was mirrored precisely by the unloading of barley stripe mosaic virus expressing the green fluorescent protein. Transverse veins were not utilized in the unloading process. The data collectively indicate a symplastic mechanism of SE unloading in the sink barley leaf.

The phenomenon of phloem unloading has been studied extensively over the last decade (for review, see Oparka, 1990; Patrick, 1990, 1997; Fisher and Oparka, 1996; Schulz, 1998), but remains a poorly understood process. During phloem unloading, assimilates carried by mass flow in the translocation stream exit the sieve element-companion cell (SE-CC) complex (SE unloading; Oparka, 1990; Patrick, 1990) and are subsequently transported through a diverse range of non-phloem tissues (post-phloem transport; Wang and Fisher, 1994; Fisher and Oparka, 1996). Evidence from several plant species suggests that a symplastic pathway of SE unloading predominates in many sink tissues, although transfer of solutes to the apoplast may occur at some point along the post-phloem pathway (Patrick, 1997). In many sinks, the SE-CC complexes of the phloem are directly linked to surrounding parenchyma elements, providing circumstantial evidence for a symplastic SE-unloading step (Fisher and Oparka, 1996). Although a complete absence of plasmodesmata invokes an apoplastic transfer step, the presence of plasmodesmata is not entirely indicative of a symplastic pathway, as some plasmodesmata appear to be non-functional (for discussion, see Van Bel and Oparka, 1995). However, physiological studies, many conducted in parallel with ultrastructural studies, have also provided evidence for symplastic SE unloading in many sink tissues (for review, see Fisher and Oparka, 1996).

In contrast to storage and reproductive sinks, the mechanism of SE unloading in developing sink leaves has received less attention. The barley (*Hordeum vulgare*) leaf has been the subject of numerous anatomical (Dannenhoffer et al., 1990; Dannenhoffer and Evert, 1994; Evert et al., 1996; Trivett and Evert, 1998) and physiological (Heldt et al., 1992; Riens et al., 1994) investigations, particularly with respect to phloem transport (Gordon et al., 1982; Anderson and Dale, 1983; Farrar and Farrar, 1985; Farrar et al., 1992). However, available data are conflicting concerning the assimilate-conducting pathways that function in the leaf.

The vascular bundles of the barley leaf, in common with those of other Poaceae, display two distinct types of SE; thick-walled SEs, which apparently lack CCs (Evert et al., 1996), and thin-walled SEs that are typically connected to CCs by pore-plasmodesma units (PPUs; see van Bel and Kempers, 1997). The functional significance of these differences in SE ultrastructure is not clear, but may reflect a division of labor between the two types of SE (Evert et al., 1996). Using a dye-coupling approach, Farrar et al. (1992) found that the fluorescent dye Lucifer Yellow, when injected into cells of the bundle sheath, apparently followed a symplastic pathway of transfer to the SEs of intermediate-sized vascular bundles. However, the specific cells in which the dye was moving could not be identified with certainty (see Evert et al., 1996). In an extensive study of plasmodesmatal frequencies in source barley leaves, Evert et al. (1996) found that in contrast to other cell types in the leaf, the thick-walled SEs and the thin-walled SE-CC complexes were virtually isolated symplastically, and suggested that phloem loading and unloading in the barley leaf must involve apoplastic mechanisms. It should be stressed, however, that Evert et al. (1996) did not

[1] This work was supported by the Scottish Executive Rural Affairs Department and Large Scale Biology Corporation.

* Corresponding author; e-mail kopark@scri.sari.ac.uk; fax 0044–01382–562426.

examine plasmodesmatal frequencies in developing sink leaves of barley. Indeed a complete symplastic isolation of the phloem of the barley leaf appears unlikely as barley is host to a range of systemic plant viruses (Jackson et al., 1991; Schenk et al., 1995).

The possibility that apoplastic phloem unloading occurs in sink leaves of some members of the Poaceae is intriguing as it suggests a major difference in the mechanism of solute unloading in grasses compared with that observed for a number of dicotyledonous species. For example, in sugar beet (Schmalstig and Geiger, 1985), tobacco (Turgeon, 1987; Ding et al., 1988; Roberts et al., 1997), and Arabidopsis (Imlau et al., 1999), available evidence points to a symplastic phloem unloading pathway, despite the fact that apoplastic loading predominates in the source leaves of these species.

In the present study we examined the pathway of phloem unloading in sink barley leaves using a combination of experimental approaches. An electron microscope analysis of plasmodesmatal frequencies revealed a distinct plasmodesmatal-mediated pathway between thick-walled SEs and adjoining cells, and also between thin-walled SE-CC complexes and surrounding cells. We also compared the unloading behavior of the fluorescent probe, carboxyfluorescein (CF), with that of a systemic virus, barley stripe mosaic virus (BSMV) tagged with the green fluorescent protein (GFP). The results demonstrate a remarkably similar pattern of symplastic unloading for solutes and virus, and implicate the involvement of thick-walled and thin-walled SEs in the unloading process.

RESULTS

Plasmodesmatal Frequencies in Sink Leaf Vascular Bundles

The barley leaf is comprised of a system of longitudinal vascular bundles interconnected by numerous transverse veins (Dannenhoffer et al., 1990). Each longitudinal bundle is surrounded by two bundle sheaths, an outer parenchymatous sheath and an inner mestome sheath (Evert et al., 1996). The distribution of individual vascular elements within the bundle was described by Evert et al. (1996) and will not be detailed here. A total of 47 intermediate and large vascular bundles from developing sink leaves were examined in the electron microscope.

In the smallest emerging sink leaves several of the conducting elements of the phloem and xylem were immature (data not shown). In older sink leaves (1.5–5 cm in length; see also Table I) most of the SEs were mature (Fig. 1, A–D). Thick-walled sieve tubes occurred adjacent to the xylem elements (Fig. 1, A–D). In the sink leaves examined several of these cells were connected to neighboring parenchyma elements by conspicuous PPUs in which a single pore led into the SE, but became branched in the wall of the adjoining cell (Fig. 1, A–C). Several of the cells connected to the thick-walled SEs in this way had distinctive characteristics of CCs, including a dense cytoplasm, numerous mitochondria, and a large conspicuous nucleus (Fig. 1B). For the purpose of plasmodesmatal counts these cells were referred to as thick-walled CCs (TCC; Table I), a designation in-

Table I. *Summary of frequency of plasmodesmata between various cell types in vascular bundles in sink leaf blades of barley*

Data are for two leaves of 5 cm in length (A) and 1.2 cm in length (B), respectively. CC, Companion cell connected to a thin-walled sieve tube; MS, mestome sheath cell; ST, thin-walled sieve tube; TCC, companion cell connected to a thick-walled sieve tube; TST, thick-walled sieve tube; VP, vascular parenchyma cell.

Interface	A				B			
	No. of PD[a]	%[b]	Wall Interface[c]	Frequency[d]	No. of PD[a]	%[b]	Wall Interface[c]	Frequency[d]
TST-TST	6	0.5	22.6	0.3	0	0.00	9.1	0.0
TST-TCC	41	3.7	74.1	0.6	26	3.4	20.0	1.3
TCC-VP	67	6.0	137.5	0.5	31	4.0	42.4	0.7
TST-VP	21	1.9	115.7	0.2	10	1.3	64.7	0.2
ST-ST	0	0.0	94.6	0.0	4	0.5	61.2	0.1
ST-CC	79	7.0	317.5	0.2	70	9.0	194.9	0.4
ST-VP	8	0.7	267.2	0.0	2	0.3	118.7	0.0
ST-MS	4	0.4	11.4	0.4	0	0.0	23.3	0.0
CC-CC	9	0.8	29.5	0.3	2	0.3	47.6	0.0
CC-VP	84	7.5	264.0	0.3	44	5.7	185.5	0.2
CC-MS	28	2.5	24.0	1.2	6	0.8	19.2	0.3
VP-VP	362	32.3	766.1	0.5	228	29.5	405.5	0.6
VP-MS	254	22.7	614.9	0.4	170	22.0	382.1	0.4
MS-MS	43	3.8	171.8	0.3	38	4.9	132.1	0.3
MS-BS	91	8.1	456.0	0.2	92	11.9	255.3	0.4
BS-BS	24	2.1	83.0	0.3	50	6.4	36.0	1.4

[a] Total number of plasmodesmata counted. [b] Percentage of total number of plasmodesmata counted. [c] Total length of shared cell wall interface in micrometers. [d] Frequency, number of plasmodesmata per micrometers shared cell wall interface.

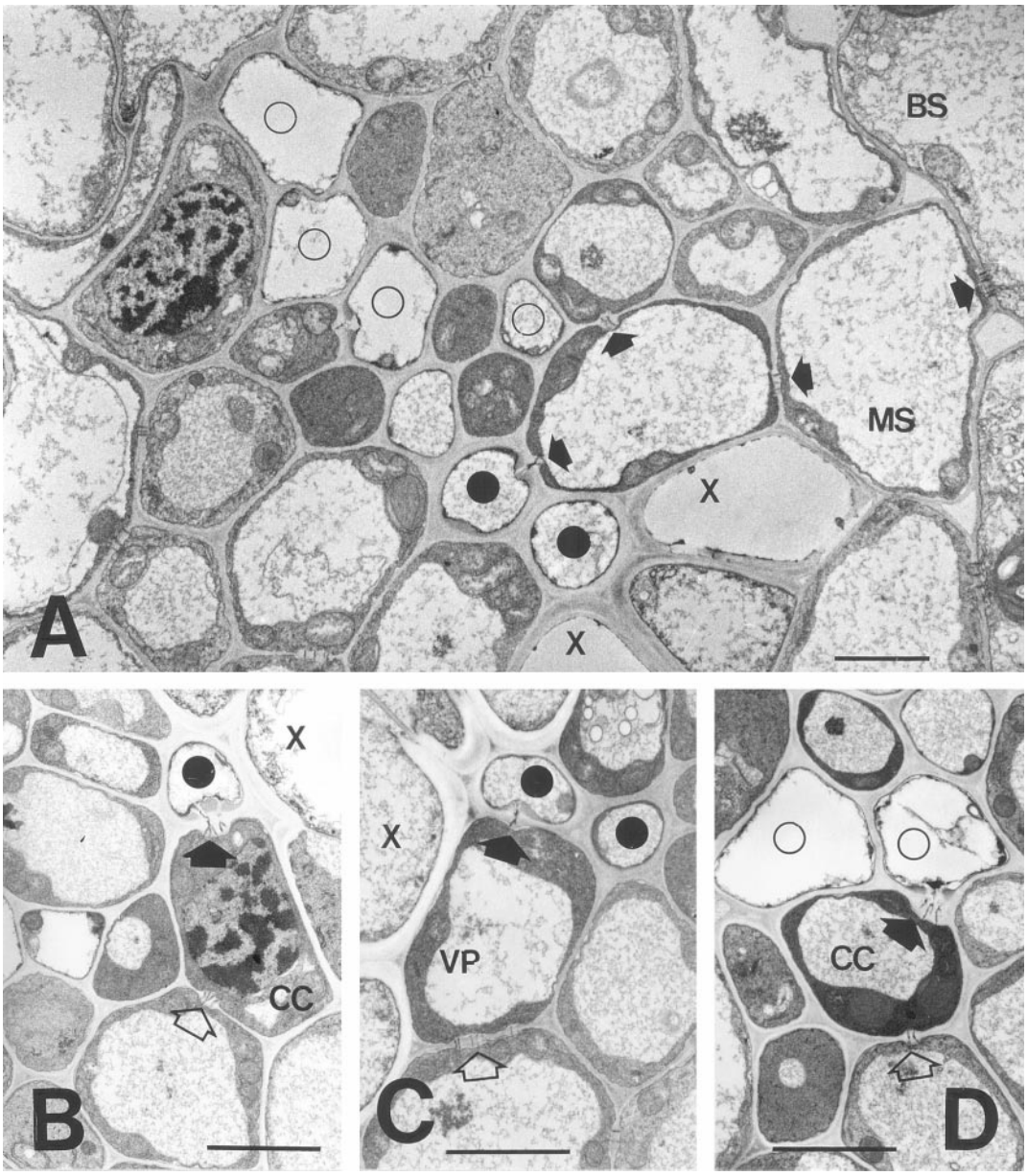

Figure 1. Electron micrographs of intermediate vascular bundles in a sink barley leaf. A, Overview of vascular bundle. Two thick-walled SEs (black circles) occur adjacent to xylem elements (X). Four thin-walled SEs (white circles) and associated CCs are also shown. A complete symplastic pathway (darts) is evident between the upper thick-walled SE and the bundle sheath (BS). Scale = 10 μm. B, Pore-plasmodesma connection between a thick-walled SE and CC (dart). Note that the CC is also connected to a vascular parenchyma element by branched plasmodesmata (white dart). Scale = 10 μm. C, Plasmodesmatal connections between a thick-walled SE and vascular parenchyma element (dart). The parenchyma element is connected to a neighboring cell by simple plasmodesmata (white darts). Scale = 10 μm. D, Pore-plasmodesma connection between a thin-walled SE and its CC (dart). The CC is in turn connected to a vascular parenchyma element (white dart). Scale = 10 μm.

tended to distinguish them from the CCs adjoined to thin-walled SEs (CC; Table I), rather than to describe their wall architecture. In other cases, the thick-walled SEs were connected by PPUs to cells that more closely resembled vascular parenchyma cell (VP; Fig. 1C; Table I).

The frequencies of plasmodesmata connecting different cells in an intermediate vascular bundle are shown diagramatically in Figure 2. When expressed on a unit-of-shared-wall basis, connections between thick walled SEs and adjoining cells were particularly abundant (Fig. 2; Table I). In turn, thick-walled CCs were connected by conspicuous fields of simple plasmodesmata to vascular parenchyma elements (Fig. 1C; Table I). The interfaces described above collectively accounted for over 17% of the total plasmodesmata counted within the vascular bundles (Table I). Direct plasmodesmal continuity between adjacent

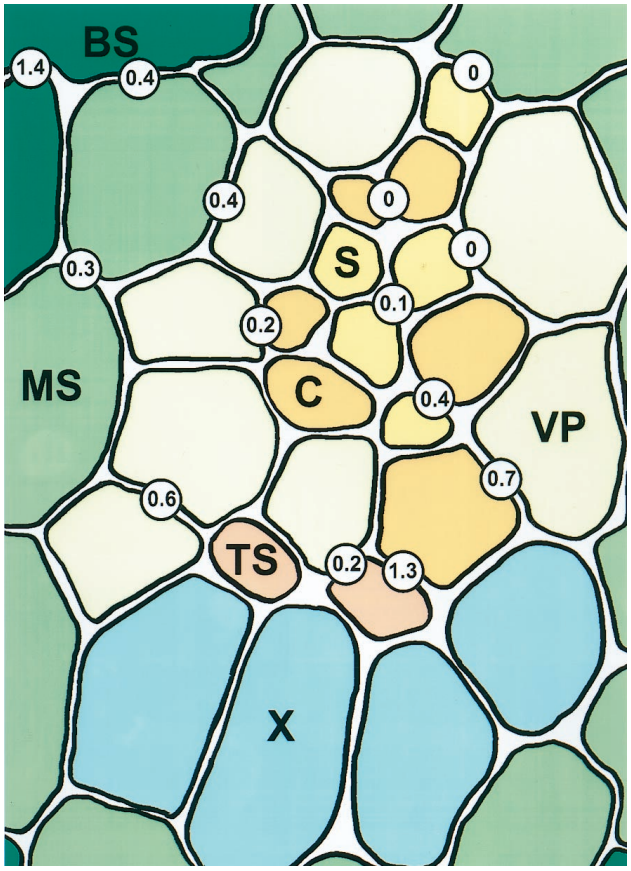

Figure 2. Diagrammatic representation of plasmodesmatal frequencies in an intermediate vascular bundle of a sink barley leaf. Values are expressed as number of plasmodesmata per micrometer of shared wall interface. BS, Bundle sheath cell; C, companion cell; MS, mestome sheath cell; S, thin-walled sieve tube; TS, thick-walled sieve tube; X, xylem.

thick-walled SEs were infrequent (Table I; Fig. 2). In the case of thin-walled SEs, which in barley are separated from the thick-walled SEs by a number of intervening vascular parenchyma elements (Evert et al., 1996), the SEs were connected to CCs by PPUs (Fig. 1D; Table I). However, the thin-walled SE-CC complexes were not symplastically isolated for source barley leaves, as demonstrated by Evert et al. (1996), and showed numerous plasmodesmatal connections to surrounding cells (Fig. 1D; Table I). Most of these occurred via the CC and connected the SE-CC complex to VPs or directly to mestome sheath cells (Fig. 1D; Table I). All of the remaining cells in the vascular bundle showed relatively high frequencies of plasmodesmata (Fig. 1A; Table I), providing evidence for a complete symplastic pathway from thick- and thin-walled SEs to the mesophyll.

Phloem Transport and Unloading of CF

When barley seedlings were labeled with CF at the three-leaf stage the dye was translocated in the phloem to emerging sink leaves. The unloading pattern across the leaf was imaged noninvasively by attaching the sink leaves of intact plants to a glass plate and observing the arrival of the dye under a confocal laser scanning microscope (CLSM). In this way real-time imaging of phloem transport was possible (see Oparka et al., 1994). CF unloading occurred only from longitudinal major veins and was extremely rapid (Fig. 3, A and B). Transverse veins did not support CF unloading (Fig. 3C). A typical unloading sequence is shown in Figure 3B. CF appeared in the sink leaf within 50 min after dye application and showed a consistently "patchy" pattern of unloading. The distribution of dye was discontinuous along the length of a single vein (Fig. 3, A and B). Within a short time period of approximately 30 s the dye was unloaded and moved laterally from the veins into subtending mesophyll tissues (Fig 3B). All cells of the importing leaf eventually became labeled with unloaded CF (Fig. 3C).

To identify the vascular bundles involved in CF import and to confirm that the CF had been translocated in the phloem, the importing leaves were detached from the plant and placed in a solution of 3-kD Texas Red dextran to label functional xylem elements. This process allowed simultaneous imaging of functional phloem and xylem within a single vascular bundle (see Roberts et al., 1997). Transverse sections through the base of double-labeled leaf blades are shown in Figure 3D. Note that in the exporting leaf CF is restricted to the vascular bundles, with little or no escape to surrounding mesophyll tissues. In contrast, within smaller sink leaves dye is distributed throughout the mesophyll tissues. In the innermost, immature sink leaves little or no dye loading was observed, and CF remained restricted to only three vascular bundles (arrows, Fig. 3D). These observations are consistent with the view that the phloem is immature in these leaves.

Images of translocating vascular bundles are shown in Figure 3E. Within a single vascular bundle not all elements of the phloem were evenly labeled with CF. Although attempts were made to prevent dye loss during tissue sectioning, we could not determine whether this uneven labeling pattern was due to dye loss from individual SE or whether some sieve tubes were not functioning in long-distance CF transport. In many cases, strong CF labeling was observed in SEs close to the xylem (Fig. 3E, i and ii), a position predicted for the location of thick-walled SEs (Figs. 1 and 2), whereas in others the CF was clearly being translocated in thin-walled SE-CC complexes (Fig. 3E, i and ii). In contrast to exporting leaves, in importing sink leaves there was a distinct labeling of surrounding mesophyll cells due to unloading of CF from the phloem (Fig. 3, C and E, iii).

Systemic Movement of BSMV.GFP

Inoculation of source barley leaves with BSMV.GFP produced fluorescent systemic symptoms on sink

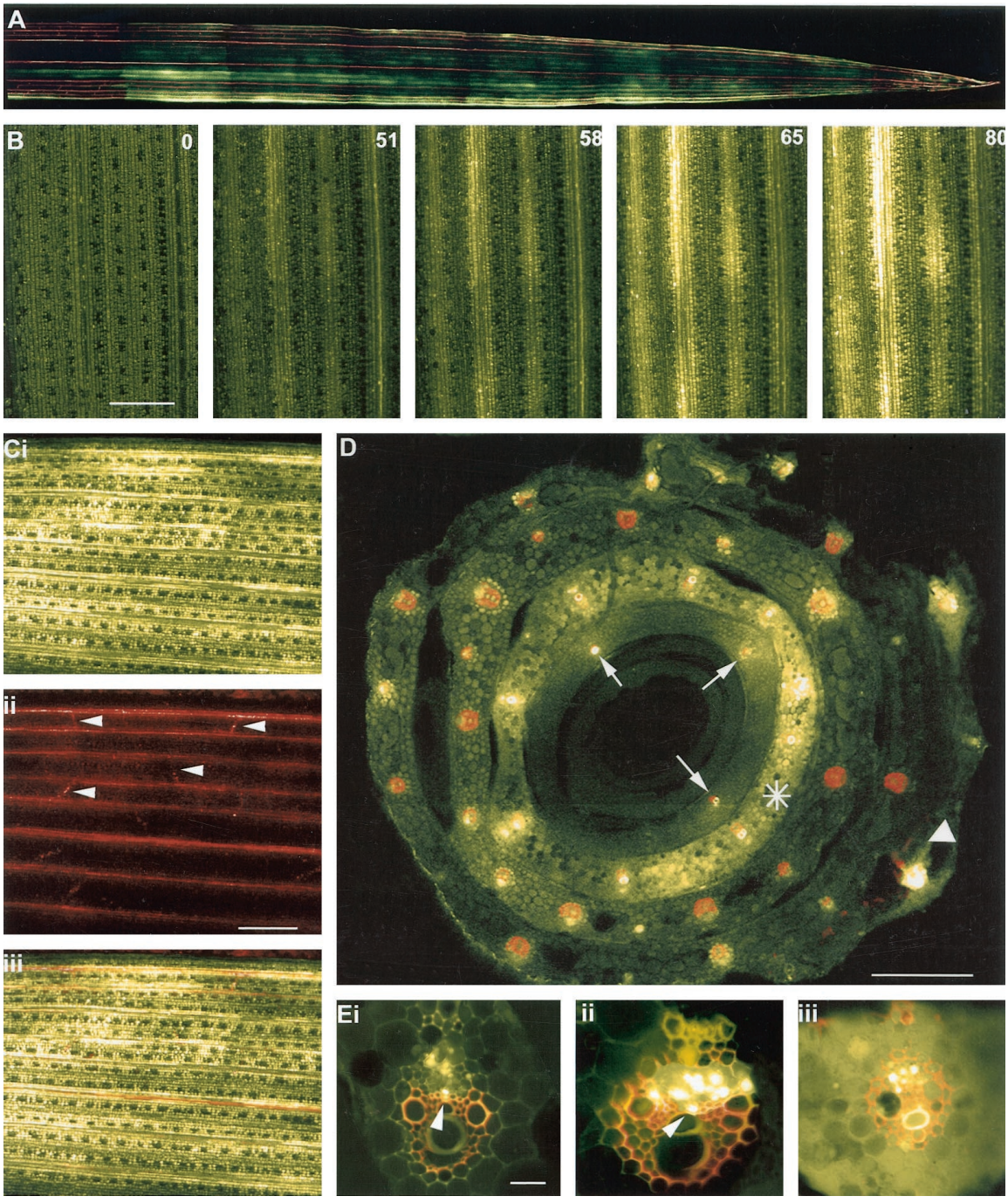

Figure 3. Unloading of CF in sink barley leaves. A, CLSM image of CF unloading in the apical region of a sink leaf of barley. Note the discontinuous exit of dye from the major vascular bundles. The functional xylem of the leaf was labeled with Texas Red dextran. The sink leaf was 5 cm long. B, CLSM imaging of the progression of CF unloading into a sink leaf of barley. The CF was first detected above background at 51 min after labeling of a source leaf. The numbers in the right-hand corner of the remaining images depict the time(s) of subsequent images of the unloading process. Note the rapidity of phloem unloading following the arrival of the dye in the leaf. A discontinuous pattern of dye unloading is also evident. Time in minutes. Scale = 1.0 mm. C, Sink leaf after unloading CF for 100 min. i, Extensive dye spread is evident from the major longitudinal bundles into the mesophyll. ii, Same region of leaf showing functional xylem stained with Texas red dextran. Lateral veins (darts) are evident. iii, Image merge of i and ii. Scale = 1.0 mm. D, CLSM image of the base of a leaf sheath following labeling of a single source leaf (white dart) with CF. Note that in the source leaf, CF is restricted to the vascular bundles. The leaf was also labeled with Texas red to depict functional xylem elements. The bulk of phloem unloading occurs from an inner sink leaf (asterisk) and dye has clearly entered the leaf mesophyll. In the innermost (immature) sink leaf dye is restricted to only three translocating vascular bundles (arrows) due to immaturity of the phloem in this leaf. Scale = 0.5 mm. E, CLSM images of vascular bundles translocating CF. In some of the vascular bundles (i and ii) labeled phloem elements occupy the position expected for thick-walled SEs (darts). iii, Vascular bundle from an unloading sink leaf. Note the presence of dye in the mesophyll. Some CF also remains present within SEs of the phloem. The functional xylem was labeled with Texas red dextran. Scale = 150 μm.

leaves within 4 to 5 d following inoculation. Although the rate of spread of virus movement on sink leaves was slow in comparison with CF, the pattern of fluorescence spread was identical; virus escape first occurred from major veins and was followed by cell-to-cell spread through mesophyll tissues (Fig. 4, A–C). As in the case of CF unloading, the exit of BSMV.GFP was discontinuous along the length of a single vein (Fig. 4, A and B). Examination of vascular bundles from systemically infected leaves revealed a number of parenchyma elements of the phloem to be infected, several of these occurring adjacent to xylem elements (Fig. 4D, i and ii). From these infected cells the virus escaped into the mesophyll and replicated extensively (Fig. 4D, ii and iii). With time, the virus entered the mesophyll tissues between veins and also infected the epidermis (Fig. 4E, i and ii).

DISCUSSION

Based on an ultrastructural study of plasmodesmatal frequencies in the leaf blade of barley, Evert et al. (1996) concluded that the barley leaf must utilize an apoplastic pathway of phloem unloading. In contrast, our observations provide strong evidence that a symplastic pathway of phloem unloading operates in the sink barley leaf. In the extensive study of Evert et al. (1996) plasmodesmatal frequencies were examined in fully expanded third or fourth leaves of barley, which almost certainly would have been exporting carbon (Anderson and Dale, 1983). From their investigation, Evert et al. (1996) noted that the thick-walled SEs and also the thin-walled SEs were symplastically isolated and concluded that symplastic phloem unloading was unlikely. Our present study of sink leaves demonstrates that plasmodesmatal connections are abundant between the above types of SE and surrounding cells and indicates that a major change occurs in plasmodesmatal distribution between the sink and source stages of barley leaf development.

In several species, apoplastic loading of solutes appears to occur in the source leaf, whereas symplastic unloading occurs in the sink leaf. For example, in tobacco, phloem loading is eliminated in the presence of the Suc carrier inhibitor, PCMBS (Turgeon, 1984). On the other hand, in the sink leaf, phloem loading is insensitive to PCMBS and anoxia, indicating a symplastic-unloading pathway (Turgeon, 1987). Such a symplastic pathway was established recently by Roberts et al. (1997) who compared the unloading of a fluorescently tagged potato virus X with CF. Virus and fluorescent solute were unloaded predominantly from class III veins, the minor veins (classes IV and V) playing no role in the unloading process. In tobacco, the minor veins become active in apoplastic solute loading following the sink/source transition (Turgeon 1984; Ding et al., 1988; Roberts et al., 1997), at which point the major veins begin to function in the export of assimilates from the leaf. For this change to occur, a down-regulation of the plasmodesmata that connected the major veins to the mesophyll must occur to allow them to function solely in export (Roberts et al., 1997). How this occurs is currently unknown, although it is possible that the plasmodesmata at these interfaces decrease in number or are lost completely during the sink/source transition (Ding et al., 1988).

Other changes in plasmodesmatal distribution during the sink source transition have been reported. In tobacco leaves, simple plasmodesmata are gradually converted to branched plasmodesmata during the sink-source transition, a feature correlated with a massive down-regulation of plasmodesmal conductance (Oparka et al., 1999). In the Cucurbitaceae, plasmodesmata between intermediary cells and bundle sheath cells increase in numbers and undergo extensive branching prior to the sink/source transition, a feature most likely associated with the symplastic mode of phloem loading adopted in this species (Volk et al., 1996). It is possible that in developing leaves of barley, as in other apoplastically loading species, that the plasmodesmata originally utilized in symplastic phloem unloading from major veins are lost during the sink/source transition, allowing a membrane-mediated mode of phloem loading to commence in the source leaf. The mechanisms by which plasmodesmata are lost or formed de novo at specific cellular interfaces during development remain poorly understood and are currently the focus of further study in our laboratory. It is clear, however, that during leaf growth, plasmodesmata are transient structures, and that plasmodesmatal frequencies at discrete cellular interfaces may become altered in a developmentally regulated pattern. Thus measurements of plasmodesmatal frequencies in mature leaves may not be applicable to earlier stages of leaf development.

The presence of thick- and thin-walled sieve tubes in grass leaves has been well documented (Fritz et al., 1983; Evert and Mierzwa, 1989), although their function remains obscure. Kuo and O'Brien (1974) suggested that thick-walled SEs in wheat may function in long-distance transport. However, subsequent autoradiographic studies showed little labeling of thick-walled SEs in translocating leaves (Cartwright et al., 1977). In a detailed study of the maize source leaf, Fritz et al. (1983) supplied radioactive Suc via the xylem and found that it was retrieved by VP and then transferred to thick-walled SEs. Supplying $^{14}CO_2$ to leaves also resulted in labeling of thick-walled SEs, but these cells, unlike their thin-walled counterparts, failed to translocate Suc out of the leaf during a subsequent chase period. The authors suggested that thick-walled SEs may function predominantly in solute retrieval from the xylem. Our data indicate that both thick- walled and thin-walled SEs

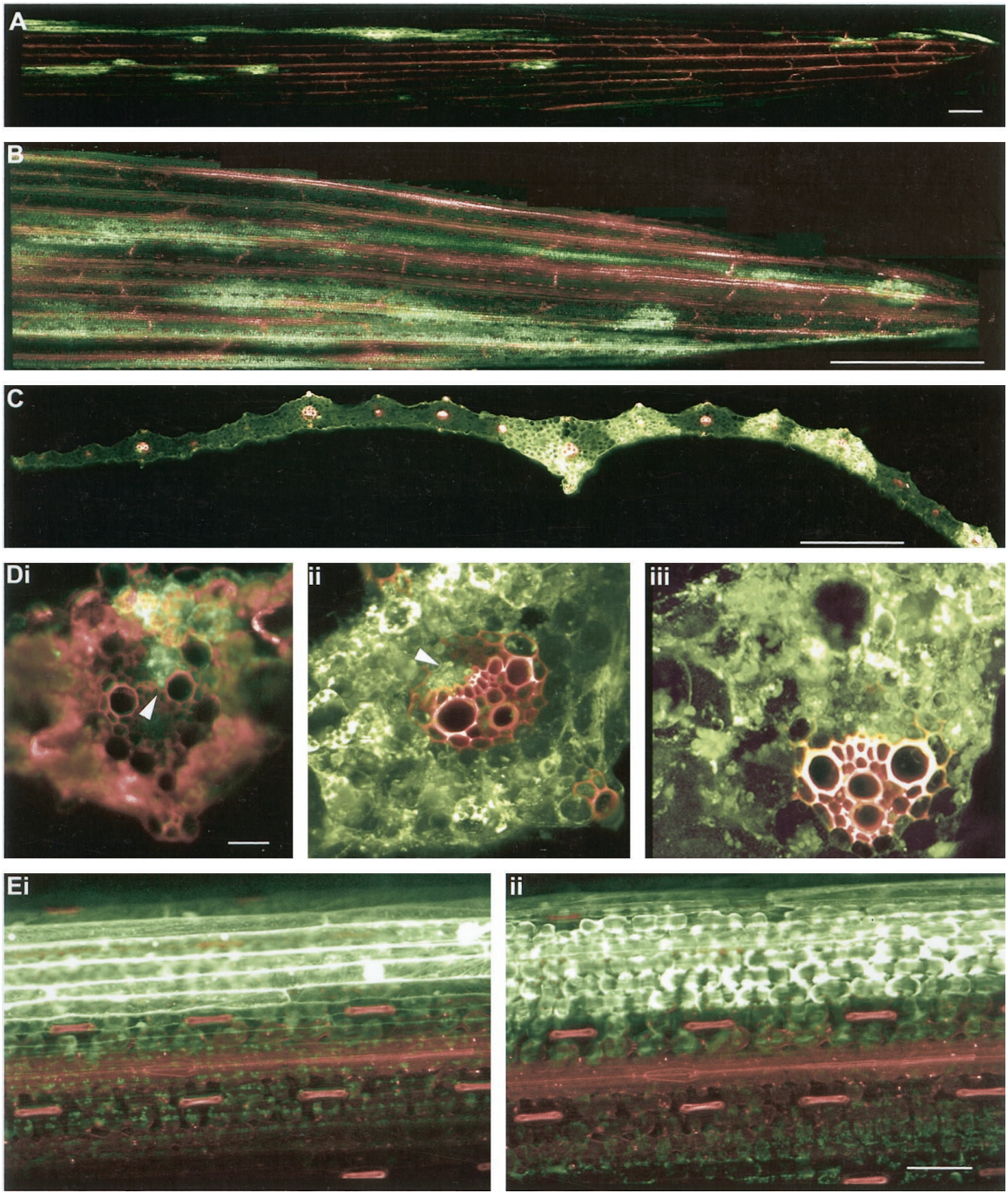

Figure 4. Systemic movement of BSMV.GFP. A, Initial unloading of the virus occurs as discrete fluorescent "flecks" from major longitudinal veins. Scale = 1.0 mm. B, With time the virus spreads from the veins into mesophyll tissues. Note the discontinuous pattern of virus exit. Scale = 0.5 cm. C, Transverse section of a sink leaf after invasion by BSMV.GFP. Note the presence of virus in mesophyll tissues adjacent to major vascular bundles. Scale = 1.0 mm. D, Progression of viral invasion from the phloem to mesophyll. i, The virus is present in phloem elements (dart) and has begun to escape to the mesophyll. ii, Later in the infection process the virus is still evident in the phloem (dart) although extensive movement to the mesophyll has now occurred. iii, Major vascular bundle showing extensive labeling of phloem and surrounding mesophyll. The xylem was labeled with Texas red dextran. Scale = 150 μm. E, Confocal images showing movement of virus into the sink-leaf epidermis. i, Optical plane is focused on the epidermis. ii, Optical plane is focused on the underlying mesophyll. Scale = 0.1 mm.

may function in the unloading process. Both types of SE were found to translocate CF and both were symplastically connected to the mesophyll via intervening cells. We found that mature thick-walled SEs were present during the early stages of leaf development. Furthermore, plasmodesmatal connections between thick-walled SEs and adjoining CCs were abundant at this early stage of leaf development (Table I). Our observations contrast with those of Evert et al. (1996) in that most of the cells connected to thick-walled SEs by PPUs had the characteristics of CCs, rather than vascular parenchyma elements. Without a CC-specific molecular marker, it is clearly difficult to identify CCs with certainty. However, our results suggest that the unloading pathway from thick-walled SEs may occur via adjoining CCs.

Extensive and rapid unloading of CF was observed from longitudinal veins, suggesting that CF unloading is unrestricted along the post-phloem pathway. In tobacco sink leaves (Oparka et al., 1999) and in developing wheat grains (Fisher and Cash-Clark, 2000), cells of the post-phloem pathway possess plasmodesmata with a high molecular size exclusion limit, facilitating rapid fluxes of solutes in these tissues. In tobacco sink leaves, macromolecular trafficking of proteins was found to be a unique feature of simple plasmodesmata, a capacity that was lost during the conversion of simple to branched plasmodesmata. It remains to be shown whether sink tissues in monocotyledonous leaves also possess a high SEL that facilitates assimilate fluxes during unloading.

Our observations for BSMV.GFP transport in sink leaves are also in agreement with a symplastic unloading pathway. Patterns of virus escape from the phloem of longitudinal veins were identical to that observed for CF. In most cases in which the mesophyll was infected, replicating virus was also detected in the phloem of the vascular bundle. However, it was impossible to determine, at the cellular level, the precise pathway of virus exit from the phloem. Studies of virus movement in sink leaves demonstrate that the pattern of virus unloading mirrors that observed for assimilates, albeit over a longer time scale (Leisner and Turgeon, 1993; Roberts et al., 1997; Oparka and Santa Cruz, 2000). The escape of BSMV.GFP from the phloem of importing barley leaves conforms to this pattern and indicates a significant capacity for symplastic transfer of BSMV RNA from the phloem to the mesophyll. In a previous study of virus unloading in tobacco (Roberts et al., 1997) it was found that minor veins played no role in virus escape, probably as these were immature in sink leaves at the time of virus entry. In the present study also, we found that virus exit occurred from relatively large vein classes. It is interesting to note that transverse veins, although functional in xylem transport during the import phase, played no role in either CF or virus unloading. The developmental state of these veins was not determined. However, our observations are consistent with the view that transverse veins may function only during the loading phase, perhaps to transfer assimilates laterally from small (loading) bundles to large (exporting) bundles, as suggested by Altus and Canny (1982).

MATERIALS AND METHODS

Plant Material

Plants of barley (*Hordeum vulgare* cv Black Hulless) were grown from seeds in a heated greenhouse and used for experiments when plants were between 2 and 3 weeks old.

Electron Microscopy

Mid-segments of the third importing sink leaves (measured acropetally) ranging from 1 to 5 cm in length were fixed in 5% (w/v) glutaraldehyde in PIPES (1,4-piperazinediethanesulfonic acid) buffer (pH 8.0) containing 1% (w/v) tannic acid for 18 h at room temperature. The segments were post-fixed in 0.2% (w/v) osmium teroxide for 72 h, dehydrated through a graded ethanol series, and embedded in Araldite resin (Agar Scientific, UK). Ultrathin sections were stained with lead citrate and uranyl acetate and viewed in an electron microscope (CM-10 TEM, Philips, Eindhoven, The Netherlands; see Roberts et al., 1997).

Counts of Plasmodesmata

Plasmodesmata frequencies were calculated using the methods described by Evert et al. (1996). Data were collected from 47 large and intermediate bundles from sink leaves ranging from 1 to 5 cm in length. Tissue was sampled from the mid-region of the expanding lamina. Only plasmodesmata extending at least as far as the middle lamella were counted. The length of shared-cell interfaces were measured from photographs and the position of individual plasmodesmata was recorded directly from the prints.

Phloem Transport and Unloading of CF

To image phloem transport and unloading, the adaxial surface of a mature source leaf was gently abraded with fine sandpaper, and 20 μL of 6(5)-CF diacetate (60 μg/mL) was applied to the leaf surface. Treated leaves were then covered with polythene film, as described in Roberts et al. (1997) to prevent evaporation of the dye. The plants were imaged after translocation in the light for between 45 and 60 min. After this period the 3rd expanding leaf was fixed to the stage of a CLSM (see below).

Xylem Transport

On several occasions, plants that had transported CF were detached and the base of the excised stem immersed immediately in a solution containing 1 mg/mL 3-kD Texas

Red dextran (Molecular Probes, Eugene, OR) to trace xylem transport. Over an uptake period of between 5 and 10 min, the 3-kD Texas Red dextran had reached the tips of transpiring leaves.

Sectioning

Prior to confocal imaging barley sink leaves and bases were cut free hand into transverse sections. The sections were then mounted immediately in silicon oil to prevent dye loss and covered with a coverslip.

Construction of the BSMV.GFP

A plasmid containing an infectious cDNA clone of the BSMV γ RNA (γ.42) was modified to express GFP as a fusion to the C-terminal of the γb protein. Site-directed mutagenesis was used to replace nucleotides 2,531 to 2,536 of γ.42 with the 6-bp recognition site of the *Nhe*I restriction endonuclease.

Oligonucleotide primers containing a *Spe*I or a *Nhe*I site were used to amplify the cycle 3 GFP open reading frame (ORF) that is brighter than wild-type GFP, but has a wild-type excitation spectra (Crameri et al., 1996). This fragment was cut with *Spe*I and *Nhe*I and inserted at the *Nhe*I site and engineered into γ42 plasmid. This fused the cycle 3 GFP ORF in frame with the 3′ end of the γb ORF.

Inoculation of Plants with BSMV.GFP

The source leaves were inoculated with RNA in a buffer containing 0.1 M Gly/phosphoric acid, pH 8.5 to 9.0, 0.06 M K_2HPO_4, 1% (w/v) sodium pyrophosphate, 1% (w/v) celite, and 1% (w/v) aluminum oxide.

CLSM

To image GFP and to follow the movement of the fluorescent probes CFDA and 3-kD Texas Red dextran, respectively, an MRC 1000 (Bio-Rad, Hemel Hempstead, UK) CLSM was used. To image intact plants, the whole plant within its pot was held on a clamp adjacent to the microscope stage. The 3rd sink leaf was than attached to a glass plate to hold it stable during the translocation process (see Oparka et al., 1994). GFP and CF were excited by the 488-nm line produced by a 25-mW krypton/argon laser, and 3-kD Texas Red dextran was excited by using green excitation (568 nm). To reconstruct the entire sink leaf, low magnification images were "mapped" using a long working distance lens (X2, Nikon, Tokyo) and the images subsequently reconstructed using Photoshop software (Adobe, Mountain View, CA).

ACKNOWLEDGMENTS

We are grateful to Andy Jackson and Diane Lawrence (University of Berkeley) for the original BSMV.GFP construct.

Received June 6, 2000; modified July 26, 2000; accepted August 16, 2000.

LITERATURE CITED

Altus DP, Canny MJ (1982) Loading of assimilates in wheat leaves: I. The specialisation of vein types for separate activities. Aust J Plant Physiol **9:** 571–581

Anderson LS, Dale JE (1983) The sources of carbon for developing leaves of barley. J Exp Bot **34:** 405–414

Cartwright SC, Lush WM, Canny MJ (1977) A comparison of translocation of labeled assimilates by normal and lignified sieve elements in wheat leaves. Planta **134:** 207–208

Crameri A, Whitehorn EA, Tate E, Stemmer WPC (1996) Improved green fluorescent protein by molecular evolution using DNA shuffling. Nat Biotechnol **14:** 315–319

Dannenhoffer JM, Ebert WJr, Evert RF (1990) Leaf vasculature in barley, *Hordeum vulgare* (Poaceae). Am J Bot **77:** 636–652

Dannenhoffer JM, Evert RF (1994) Development of the vascular system in the leaf of barley (*Hordeum vulgare*). Int J Plant Sci **155:** 143–157

Ding B, Parthasarathy MV, Niklas K, Turgeon R (1988) A morphometric analysis of the phloem-unloading pathway in developing tobacco leaves. Planta **176:** 307–318

Evert RF, Mierzwa RJ (1989) The cell wall plasmalemma interface in sieve tubes in barley. Planta **177:** 24–34

Evert RF, Russin WA, Botha CEJ (1996) Distribution and frequency of plasmodesmata in relation to photoassimilate pathway and phloem loading in the barley leaf. Planta **198:** 572–579

Farrar J, van der Schoot C, Drent P, van Bel AJE (1992) Symplastic transport of Lucifer Yellow in mature leaf blades of barley: potential mesophyll-to-sieve-tube transfer. New Phytol **120:** 191–196

Farrar SC, Farrar JF (1985) Carbon fluxes in leaf blades of barley. New Phytol **100:** 271–283

Fisher DB, Cash Clark,C (2000) Sieve tube unloading and post-phloem transport of fluorescent tracers and proteins injected into sieve tubes via severed aphid stylets. Plant Physiol (in press)

Fisher DB, Oparka KJ (1996) Post-phloem transport: principles and problems. J Exp Bot **47:** 1141–1154

Fritz E, Evert RF, Heyser W (1983) Microautoradiographic studies of phloem loading and transport in the leaf of *Zea mays*. Planta **159:** 193–206

Gordon AJ, Ryle GJA, Mitchell DF, Powell CE (1982) The dynamics of carbon supply from leaves of barley plants grown in long or short days. J Exp Bot **33:** 241–250

Heldt HW, Lohaus G, Winter H (1992): Phloem transport of amino-acids and sucrose in relation to their cytosolic levels in barley leaves. Photosynth Res **34:** 241

Imlau A, Truenit E, Sauer N (1999) Cell-to-cell and long-distance trafficking of the green fluorescent protein in the phloem and symplastic unloading of the protein into sink tissue. Plant Cell **11:** 309–322

Jackson AO, Petty IDT, Jones RW, Edwards MC, French R (1991) Molecular genetic-analysis of barley stripe

mosaic-virus pathogenicity determinants. Can J Plant Pathol **13:** 163–177

Kuo J, O'Brien TP (1974) Lignified sieve elements in the wheat leaf. Planta **117:** 349–353

Leisner SM, Turgeon R (1993) Movement of virus and photoassimilate in the phloem: a comparative analysis. Bioessays **15:** 741–748

Oparka KJ (1990) What is phloem unloading? Plant Physiol **94:** 393–396

Oparka KJ, Duckett CM, Prior DAM, Fisher DB (1994) Real-time imaging of phloem unloading in the root tip of *Arabidopsis*. Plant J **6:** 756–766

Oparka KJ, Roberts AG, Boevink P, Santa Cruz S, Roberts I, Pradel KS, Imlau A, Kotlizky G, Sauer N, Epel B (1999) Simple, but not branched, plasmodesmata allow the non-specific trafficking of protein in developing tobacco leaves. Cell **97(6):** 743–754

Oparka KJ, Santa Cruz S (2000) The great escape: phloem transport and unloading of macromolecules. Annu Rev Plant Physiol Plant Mol Biol (in press)

Patrick JW (1990) Sieve element unloading: cellular pathways, mechanisms and control. Physiol Plant **78:** 298–308

Patrick JW (1997) Phloem unloading: sieve element unloading and post-sieve element transport. Annu Rev Plant Physiol **48:** 191–222

Riens B, Lohaus G, Winter H, Heldt HW (1994) Production and diurnal utilization of assimilates in leaves of spinach (*Spinacia oleracea* L.) and barley (*Hordeum vulgare* L.). Planta **192:** 497–501

Roberts AG, Santa Cruz S, Roberts IM, Prior DAM, Turgeon R, Oparka KJ (1997) Phloem unloading in sink leaves of *Nicotiana benthamiana*: comparison of a fluorescent solute with a fluorescent virus. Plant Cell **9:** 1381–1396

Schenk PM, Antoniw JF, Batista MD, Jacobi V, Adams MJ, Steinbiss HH (1995) Movement of *barley mild mosaic* and *barley yellow mosaic-viruses* in leaves and roots of barley. Ann Appl Biol **126:** 291–305

Schmalstig JG, Geiger DR (1985) Phloem unloading in developing leaves of sugar beet. Plant Physiol **79:** 237–241

Schulz A (1998) Phloem: structure related to function. Prog Bot **59:** 430–477

Trivett CL, Evert RF (1998) Ontogeny of the vascular bundles and contiguous tissues in the barley leaf blade. Int J Plant Sci **159:** 716–723

Turgeon R (1984) Termination of nutrient import and development of vein loading capacity in albino tobacco leaves. Plant Physiol **76:** 45–48

Turgeon R (1987) Phloem unloading in tobacco sink leaves: insensitivity to anoxia indicates a symplastic pathway. Planta **171:** 73–81

van Bel AJE, Kempers R (1997) The pore/plasmodesm unit: key element in the interplay between sieve element and companion cell. Prog Bot **58:** 277–291

van Bel AJE, Oparka KJ (1995) On the validity of plasmodesmograms. Bot Acta **108:** 174–182

Volk GM, Turgeon R, Beebe DU (1996) Secondary plasmodesmata formation in minor-vein phloem of *Cucumis melo* L. and *Cucurbita pepo* L. Planta **199:** 425–432

Wang N, Fisher DB (1994) The use of fluorescent tracers to characterize the post-phloem transport pathway in maternal tissues of developing wheat grains. Plant Physiol **104:** 17–27